Published in final edited form as:
Adv Mater. 2009 April 6; 21(13): 1344–1348. doi:10.1002/adma.200803053.

Photonic Shell-Crosslinked Nanoparticle Probes for Optical Imaging and Monitoring**

Nam S. Lee,
Departments of Chemistry and Radiology, Washington University in Saint Louis, Saint Louis, MO 63130 (USA)

Guorong Sun,
Departments of Chemistry and Radiology, Washington University in Saint Louis, Saint Louis, MO 63130 (USA)

Dr. William L. Neumann,
Covidien Imaging Solutions R&D, 675 McDonnell Blvd., Hazelwood, MO 63042 (USA)

Dr. John N. Freskos,
Covidien Imaging Solutions R&D, 675 McDonnell Blvd., Hazelwood, MO 63042 (USA)

Dr. Jeng J. Shieh,
Covidien Imaging Solutions R&D, 675 McDonnell Blvd., Hazelwood, MO 63042 (USA)

Dr. Richard B. Dorshow, and
Covidien Imaging Solutions R&D, 675 McDonnell Blvd., Hazelwood, MO 63042 (USA)

Karen L. Wooley[Prof.]
Departments of Chemistry and Radiology, Washington University in Saint Louis, Saint Louis, MO 63130 (USA)

Karen L. Wooley: klwooley@wustl.edu

Abstract

**Financial support from Covidien is gratefully acknowledged. This material is based upon work supported partially also by the National Heart, Lung and Blood Institute of the National Institutes of Health as a Program of Excellence in Nanotechnology (HL080729). Supporting Information is available online from Wiley InterScience or from the author.

Correspondence to: Karen L. Wooley, klwooley@wustl.edu.

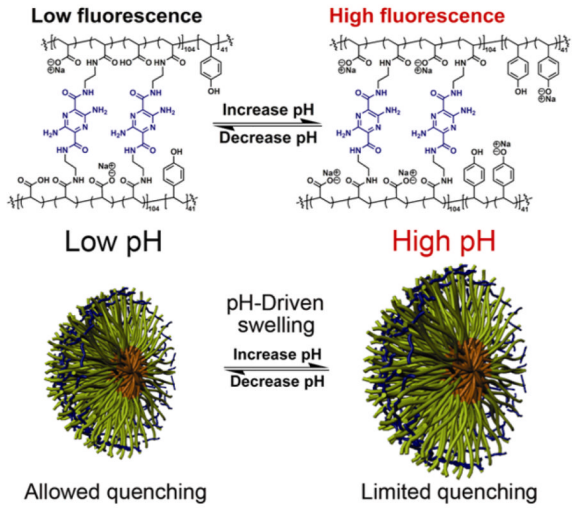

A pH-insensitive fluorophore is made to give pH-driven responses through its covalent incorporation within a nanostructure derived from pH-responsive polymers. Fluorophore-shell-crosslinked nanoparticles (SCKs) demonstrate notable enhancement of photophysical properties, in the physiological pH region. Fluorophore-SCKs are designed to swell at higher pH and shrink as the pH is lowered, producing high fluorescence *vs*. low fluorescence outputs, respectively.

Keywords

Biomedical Materials; Optically Active Materials; Photonics; pH-Responsive Nanoparticles; Polymeric Materials

---

Although fluorescence changes in response to pH is a common phenomenon, we have designed a unique system that relies upon pH-non-responsive probe molecules to serve as stabilizers for nanoscale objects that then impart pH-driven fluorescence emission responses. Without the fluorogenic probe-based crosslinks, the nanostructures would disintegrate at elevated pH values, and without the internal nanostructure environment, the fluorogenic probe affords no pH responsive characteristics. These combined effects take place within the shell layers of block copolymer micelles.

Shell-crosslinked micelles have been shown to be excellent nanostructural platforms for a variety of biomedical applications, ranging from the delivery of large payloads of chemotherapeutics and diagnostic agents to the *in vivo* targeting of such entities to tumors *via* the external multivalent presentation of tissue specific ligands.[1–3] The outstanding versatility of these systems is derived from both the ease with which they are produced (by placing amphiphilic block copolymers into a solvent that is selective for solubilizing a portion of the polymer chain segments), and the final core-shell or other (multi) compartment-type morphologies.[4–10] In general, for shell-crosslinked knedel-like (SCK) nanoparticles derived from amphiphilic block copolymers containing poly(acrylic acid) as the hydrophilic, crosslinkable component, non-functional diamines have been used to chemically crosslink the carboxylate-rich shells in order to generate stable discrete nanoparticles.[11] Even in cases where the core domain is transformed from a hydrophobic block copolymer segment to a hydrophilic polymer chain or degraded into small molecule fragments through chemical excavation strategies, the covalently-crosslinked shell layer retains structural integrity, resulting in the formation of nanocage frameworks, which are able to undergo expansion and contraction under changing environmental conditions.[4]

We have used the reversible hydrophobicity/hydrophilicity of the core domain to drive the block copolymer micelle assembly/disassembly in water without the aid of organic solvents, as a convenient approach to the formation of SCKs with the retention of chemically functional groups in the core and the shell.[12–15] In this pursuit, we also realized that simple polymer nanoparticles could be fashioned into sophisticated sensing devices,[16–18] by bringing together the concepts of reversible hydrophobicity and nanoparticle expansion/contraction, with the use of functional crosslinkers. The functional crosslinkers provide structural integrity and optical signals to both mediate and probe the local changes within the SCKs, promoted by tuning the pH of the aqueous solution. Herein, we report notable enhancement of photophysical properties for fluorophore-shell-crosslinked nanoparticles (fluorophore-SCKs), as a result of changing the pH across the physiological range. The current systems have been designed to produce high fluorescence when the shell is swollen at elevated pH and to allow for fluorescence quenching when the shell shrinks as the pH is lowered (Fig. 1). It has been demonstrated that the covalent attachment of fluorogenic crosslinkers within the SCK shell provides this behavior uniquely.

The micellar precursors to the fluorophore-SCKs were assembled from the diblock copolymer, poly(acrylic acid)$_{104}$-*b*-poly(*p*-hydroxystyrene)$_{41}$, PAA-*b*-P*p*HS (**1**), which was synthesized *via* nitroxide-mediated radical polymerization.[19] Micelles were formed by first dissolving the block copolymer in water at high pH (pH = 12) and then slowly decreasing the solution pH to 7, at which the protonated P*p*HS blocks nucleated to form hydrophobic core domains while maintenance of the deprotonated PAA block constituted the hydrophilic shells (Scheme 1).

The resulting micelle solution **2** was incubated with 6.25 mol% or 12.5 mol% of the diamino-terminated pyrazine, relative to the acrylic acid residues, followed by the addition of EDCI, to afford SCK **3** or **4** having different amounts of fluorophores incorporated into the shells and, therefore, different degrees of crosslinking. These 3,6-diamino-2,5-pyrazine dicarboxylic acid derivatives are bright, low molecular weight, bifunctional fluorophores emitting in the green to orange region of the electromagnetic spectrum.[20] The reaction mixtures were dialyzed against nanopure water for 4 days to remove the urea by-products and any nonattached pyrazine fluorophores. The SCK dimensions were then measured by atomic force microscopy (AFM) and transmission electron microscopy (TEM). The AFM-measured heights were observed to be 6 ± 2 nm and 8 ± 2 nm, and their TEM-measured diameters were 9 ± 2 nm and 9 ± 2 nm for SCKs **3** and **4**, respectively. Dialysis of the SCK solutions against nanopure water (*ca*. pH 7) for 3 days and then partitioning into six vials, each containing 5 mL of 5 mM PBS at pH 4.5, 6.1, 8.0, 9.5, or 11.0, placed the SCKs into different pH environments for analysis of the effects on the SCK hydrodynamic diameters and on the fluorophore photophysical properties.

As the SCK solution pH increases, two factors play major roles in expansion of the nanoparticles: 1) as more poly(acrylic acid) blocks become deprotonated, negatively-charged carboxylates repel PAA chains from one another within the confined SCK structure; 2) as the P*p*HS blocks become deprotonated at higher pH (*i.e.*, >10), the hydrophilicity of the P*p*HS core increases, allowing water molecules to enter the shell-crosslinked nanoparticles. It was hypothesized that the acrylamide-pyrazine linkages would then be able to respond to the SCKs' dual shell and core pH-driven expansion mechanisms by fluorescing upon loss of self-attractive interactions, such as hydrogen bonding, hydrophobic effects, and pi-stacking, but suffer fluorescence quenching as self-associations re-establish at lower pH values (Figure 1). Due to their D_{2h} symmetry, 3,6-diamino-2,5-diamide substituted pyrazines are quadrupolar dyes displaying photophysical characteristics that are fairly insensitive to pH changes. Thus, the resulting photophysical changes are imposed by the nanostructure.

Covalent crosslinking between the pyrazine units and the PAA shells, thereby, affords photonic SCKs for potential pH sensing. We expected to observe the photophysical consequences of the deprotonated PAA shell from pH 4.5 to 9.5 and those of the P*p*HS core from pH 9.5 to 11. In order to test our hypothesis, UV-vis and fluorescence measurements were collected on the resulting SCK solutions over the pH range of 4.5 to 11.0 to determine the pyrazine concentration, and then the concentration was normalized relative to the fluorescence intensity values (Fig. 2). To observe the photophysical properties of the photonic SCKs, the data for the pyrazines within the SCK shell layers were compared between the two SCKs having different degrees of pyrazine loading and also against the pyrazine crosslinker associated physically with PAA and as a small molecule in buffered solutions.

The UV-vis and fluorescence data support the hypothesis that expansion of the fluorophore-SCKs as a function of pH provides a unique local environment to mediate the fluorescence outputs. The UV-vis measurements of **3** and **4** indicated no significant variation among data sets, confirming consistent amounts of pyrazine loading in each sample. There was an order of magnitude greater fluorescence emission intensity, however, for **3** *vs*. **4** (Fig. 2), suggesting that a limited amount of the fluorophore-based crosslinkers can be accommodated within the SCK shell domain while avoiding fluorescence quenching, over all of the pH values studied.

Dynamic light scattering data (Fig. 3) further supported this suggestion, as the variability in the SCK hydrodynamic diameter was reduced at the higher theoretical crosslinking density (12.5 mol% fluorophore for **4**), whereas the lower theoretical degree of crosslinking (6.25 mol% fluorophore for **3**) allowed for significant shell and core expansion with increasing pH (Figure 3). The most notable enhancement in fluorescence occurred from pH 6.1 to 8.0 (Table 1), the physiologically-relevant pH range. It was also on going from pH 6.1 to 8.0 that the hydrodynamic diameter of the SCKs increased by the greatest amount. At lower pH, there is some degree of particle-particle aggregation and at higher pH, both the shell carboxylates and core phenolates contributed to the expansion within the SCKs.

Only when covalently linked within the SCK shell did the pyrazine fluorophores experience an increase in fluorescence emission with increasing pH. As illustrated in Figure 4, the pyrazine crosslinker as a small molecule in solution or in the presence of PAA underwent no change in fluorescence intensity or gave a slight decrease in intensity on increasing from pH 4.5 to 6.1 and another decrease in intensity on increasing to pH 8.0, where it remained constant until pH 11.0 at which a slight fluorescence intensity increase was observed. In contrast, significant increases in fluorescence emission were observed for the pyrazines in **3** (Table 1), *ca*. 330% increase over the pH range where expansion of the shell is expected due to deprotonation of residual acrylic acid residues, and *ca*. 370% fluorescence increase with deprotonation of the phenolic groups and expansion of the core domain, each relative to the fluorescence intensity observed at pH 4.5. The higher theoretical degree of crosslinking and higher loading of pyrazine of **4** limited the nanostructure expansion and promoted pyrazine-pyrazine fluorescence quenching, which together reduced the observed effects on fluorescence intensity (Fig. 4 and Table 1).

Thus, we have utilized a pH-insensitive fluorophore to generate a pH-sensing assembly through its covalent incorporation within a nanostructure derived from pH-responsive polymers. The bifunctional fluorophore could then be described as a photonic linkage system for the shell-crosslinking step in SCK formation. Dynamic light scattering data have shown that the hydrodynamic diameter of the fluorophore-SCKs respond to pH (swell at high pH and shrink at low pH) through the incorporation of functionality of differential pK_a (*i.e*. phenols/carboxylic acids). Photophysical consequences of these changes in

hydrodynamic diameter were manifested as “high fluorescence” at higher pH values and “low fluorescence” at lower pH values, due to quenching. The photonic SCKs’ ability to enhance the photophysical properties of the pyrazine molecules near the physiological pH region warrants further studies to incorporate a larger library of dyes as well as polymeric constituents. Potential biomedical uses for these new photonic nanosystems include chemical or physiological sensors, among other applications.

Experimental

Synthesis of poly(*tert*-butyl acrylate)$_{104}$ (5)

To a flame-dried 50-mL Schlenk flask equipped with a magnetic stir bar and under N_2 atmosphere, at room temperature (rt), was added 2,2,5-trimethyl-3-(1’-phenylethoxy)-4-phenyl-3-azahexane (600 mg, 1.84 mmol), 2,2,5-trimethyl-4-phenyl-3-azahexane-3-nitroxide (20.0 mg, 0.092 mmol), and *tert*-butyl acrylate (31.5 g, 245 mmol). The reaction flask was sealed and stirred 10 min at rt. The reaction mixture was degassed through three cycles of freeze-pump-thaw. After the last cycle, the reaction mixture was recovered back to rt and stirred for 10 min before being immersed into a pre-heated oil bath at 125 °C to start the polymerization. After 72 h, ^{1}H NMR analysis showed 72% monomer conversion had been reached. The polymerization was quenched by quick immersion of the reaction flask into liquid N_2. The reaction mixture was dissolved in THF and precipitated into H_2O/MeOH (v:v, 1:4) three times to afford white powder, (19.3 g, 85% yield based upon monomer conversion); $M_{n,GPC}$ = 13,700 Da, PDI = 1.1, DP of *tert*-butyl acrylate= 104.

Synthesis of poly(*tert*-butylacrylate)$_{104}$-*b*-poly(acetoxystyrene)$_{41}$ (6)

To a flame-dried 50-mL Schlenk flask equipped with a magnetic stir bar and under N_2 atmosphere at rt, **5** (3.0 g, 0.22 mmol) and 4-acetoxystyrene (4.44 g, 27.4 mmol) were added. The reaction mixture was allowed to stir for 1 h at rt to obtain a homogenous solution. The reaction mixture was degassed through three cycles of freeze-pump-thaw. After the last cycle, the reaction mixture was recovered back to rt and stirred for 10 min before being immersed into a pre-heated oil bath at 125 °C to start the polymerization. After 6 h, 32% monomer conversion was reached, as analyzed by ^{1}H NMR spectroscopy. After quenching by immersion of the reaction flask into a bath of liquid N_2, THF was added to the reaction mixture and the polymer was purified by precipitating into H_2O/MeOH (v:v, 1:4) three times to afford **6** as a white powder, (3.73 g, 83 % yield); $M_{n,GPC}$ = 17,400 Da, PDI = 1.3, DP of acetoxystyrene = 41.

Preparation of poly(*tert*-butyl acrylate)$_{104}$-*b*-poly(p-hydroxystyrene)$_{41}$ (7)

To a 25-mL round bottom (RB) flask, (**6**) (3.0 g, 0.15 mmol) and MeOH (10 mL) were added and stirred 10 min at rt. The cloudy mixture was heated slowly to reflux. Immediately after the solution turned clear, a sodium methoxide solution in MeOH (25 wt%) (26 mg, 0.12 mmol) was added through syringe. The reaction mixture was further allowed to heat at reflux for 4 h. After cooling down to rt, the reaction mixture was precipitated in water with 4% acetic acid to afford **7** as white solid (2.6 g, 95 % yield). $M_{n,NMR}$ = 18,600 Da.

Synthesis of poly(acrylic acid)$_{104}$-*b*-poly(*p*-hydroxystyrene)$_{41}$ (1)

To a 50 mL RB flask equipped with a stir bar, was added **7** (2.5 g, 0.13 mmol) and trifluoroacetic acid (20.2 g, 177 mmol). The reaction mixture was allowed to stir for 24 h at rt. Excess acid was removed under vacuum. The residue was dissolved into 10 mL of THF and purified by dialysis against nanopure water (18.0 MΩ-cm) for three days and freeze-dried to afford **1** as a white powder (1.6 g, 95 % yield). $M_{n,NMR}$ = 12,000 Da

Preparation of micelle 2 from 1

To a 50 mL of RB flask equipped with a magnetic stir bar was added **1** (2.0 mg, 0.16 μmol) and 15 mL of nanopure water. The pH value was adjusted to 12 by adding 1.0 M NaOH solution to afford a clear solution. The micellization was initiated after decreasing the pH value to 7 by adding dropwise 1.0 M HCl. After further stirring 12 h at rt, the micelle solution was used directly for construction of SCK **3** and **4**.

Preparation of shell-crosslinked nanoparticles (SCK 3 or 4) from micelle 2

To a 50 mL RB flask equipped with a magnetic stir bar was added a solution of micelles in nanopure H_2O (15.0 mL, 0.016 mmol of carboxylic acid residues). To this solution, was added a solution of 3,6-diamino-N^2,N^5-bis(2-aminoethyl)pyrazine-2,5-dicarboxamide (0.397 mg, 1.12 μmol (6.25 mol% relative to the acrylic acid residues) for 12.5% crosslinking extent; or 0.794 mg, 2.24 μmol (12.5 mol% relative to the acrylic acid residues) for 25% crosslinking extent) in 1 mL nanopure H_2O. The reaction mixture was allowed to stir for 2 h at rt. To this solution was added, dropwise *via* a syringe pump over 1 h, a solution of 1-[3'-(dimethylamino)propyl]-3-ethylcarbodiimide methiodide (EDCI, 0.849 mg, 2.86 μmol for 12.5% crosslinking extent; or 1.70 mg, 5.72 μmol for 25% crosslinking extent) in nanopure H_2O (1.0 mL) and the reaction mixture was further stirred for 16 h at rt. Finally, the reaction mixture was transferred to presoaked dialysis tubing (MWCO *ca*. 3,500 Da) and dialyzed against nanopure water for 3 d to remove the small molecule starting materials and by-products, and afford aqueous solutions of SCK **3** and **4**. SCK solutions for DLS, UV-vis, and fluorescence studies were further partitioned into six vials each containing 5 mM PBS (with 5 mM NaCl) at pH values of 4.5, 6.1, 8.0, 9.5, and 11.

Synthesis of 3,6-diamino-N^2,N^5-bis(2-aminoethyl)pyrazine-2,5-dicarboxamide

A mixture of sodium 3,6-diaminopyrazine-2,5-dicarboxylate (500 mg, 2.07 mmol), *tert*-butyl 2-aminoethylcarbamate (673 mg, 4.20 mmol), HOBt (836 mg, 5.46 mmol) and EDCI (1.05 g, 5.48 mmol) in DMF (25 mL) was allowed to stir for 16 h and was then concentrated. The residue was partitioned with 1 N $NaHSO_4$ (200 mL) and EtOAc (200 mL). The organic layer was separated and washed with water (200 mL × 3), sat. $NaHCO_3$ (200 mL × 3) and brine. Dried with $MgSO_4$, filtered and concentrated to afford the bisamide as an orange foam. 770 mg, 76% yield. ^{1}H NMR (300 MHz, DMSO-d_6, δ): major conformer, 8.44 (t, J = 5.7 Hz, 2 H), 6.90 (t, J = 5.7 Hz, 2 H), 6.48 (br, 4 H), 2.93–3.16 (m, 8 H), 1.37 (s, 9 H), 1.36 (s, 9 H). ^{13}C NMR (75 MHz, DMSO-d_6, δ): 165.1, 155.5, 155.4, 146.0, 126.2, 77.7, 77.5, 45.2, 44.5, 28.2. LC-MS (15–95% gradient acetonitrile in 0.1% TFA over 10 min), single peak retention time = 7.18 min on 30 mm column, $(M+H)^+$ = 483 amu. To the product (770 mg, 1.60 mmol) in methylene chloride (100 mL), was added TFA (25 mL) and the reaction was stirred at room temperature for 2 h. The mixture was concentrated and the residue was dissolved into methanol (15 mL). Diethyl ether (200 mL) was added and the orange solid precipitate was isolated by filtration and dried at high vacuum to afford an orange powder. 627 mg, 77% yield. ^{1}H NMR (300 MHz, DMSO-d_6, δ): 8.70 (t, J = 6 Hz, 2 H), 7.86 (br, 6 H), 6.50 (br, 4 H), 3.46–3.58 (m, 4 H), 3.26–3.40 (m, 4 H); ^{13}C NMR (75 MHz, DMSO-d_6, δ): 166.4, 146.8, 127.0, 39.4, 37.4. LC-MS (15–95% gradient acetonitrile in 0.1% TFA over 10 min), single peak retention time = 2.60 min on 30 mm column, $(M+H)^+$ = 283 amu. UV-vis (100 μM in PBS): λ_{abs} = 435 nm. Fluorescence (100 nM): λ_{ex} = 449 nm, λ_{em} = 562 nm. The product was converted to the HCl salt by co-evaporation (3 × 100 mL) with 1 N aqueous HCl.

References

1. O'Reilly RK, Hawker CJ, Wooley KL. Chem. Soc. Rev. 2006; 35:1068–1083. [PubMed: 17057836]

2. Xu J, Sun G, Rossin R, Hagooly A, Li Z, Fukukawa K, Messmore BW, Moore DA, Welch MJ, Hawker CJ, Wooley KL. Macromolecules. 2007; 40:2971–2973. [PubMed: 18779874]
3. Li, Y.; Sun, G.; Xu, J.; Wooley, KL. Nanotechnology in Therapeutics: Current technology and applications. Zach Hilt, J.; Brock Thomas, J.; Peppas, Nicholas A., editors. Wymondham, UK: Horizon Bioscience; 2007. p. 381-407.
4. Ma Q, Remsen EE, Kowalewski T, Schaefer J, Wooley KL. Nano Lett. 2001; 1:651–655.
5. Liu S, Armes SP. Angew. Chem. Int. Ed. 2002; 41:1413–1416.
6. Hamley IW. Nanotechnology. 2003; 14:R39–R54.
7. Li Z, Kesselman E, Talmon Y, Hillmyer MA, Lodge TP. Science. 2004; 306:98–101. [PubMed: 15459387]
8. Binks BP, Murakami R, Armes SP, Fujii S. Angew. Chem. Int. Ed. 2005; 44:4795–4798.
9. Cui H, Chen Z, Zhong S, Wooley KL, Pochan DJ. Science. 2007; 317:647–650. [PubMed: 17673657]
10. Walther A, Goldmann AS, Yelamanchili RS, Drechsler M, Schmalz H, Eisenberg A, Müller AHE. Macromolecules. 2008; 41:3254–3260.
11. Huang H, Kowalewski T, Remsen EE, Gertzmann R, Wooley KL. J. Am. Chem. Soc. 1997; 119:11653–11659.
12. Liu S, Armes SP. Angew. Chem., Int. Ed. 2002; 41:1413–1416.
13. Oishi M, Kataoka K, Nagasaki Y. Bioconjugate Chem. 2006; 17:677–688.
14. Rodríguez-Hernández J, Lecommandoux S. J. Am. Chem. Soc. 2005; 127:2026–2027. [PubMed: 15713063]
15. Lee NS, Li Y, Ruda CM, Wooley KL. Chem. Commun. 2008; 42:5339–5341.
16. Alexeev VL, Sharma AC, Goponenko AV, Das S, Lednev IK, Wilcox CS, Finegold DN, Asher SA. Anal. Chem. 2003; 75:2316–2323. [PubMed: 12918972]
17. Xu X, Goponenko AV, Asher SA. J. Am. Chem. Soc. 2008; 130:3113–3920. [PubMed: 18271586]
18. Burns A, Ow H, Wiesner U. Chem. Soc. Rev. 2006; 35:1028–1042. [PubMed: 17057833]
19. Benoit D, Chaplinski V, Braslau R, Hawker CJ. J. Am. Chem. Soc. 1999; 121:3904–3920.
20. Shirai K, Yanagisawa A, Takahashi H, Fukunishi K, Matsuoka M. Dyes Pigm. 1998; 39:49–68.

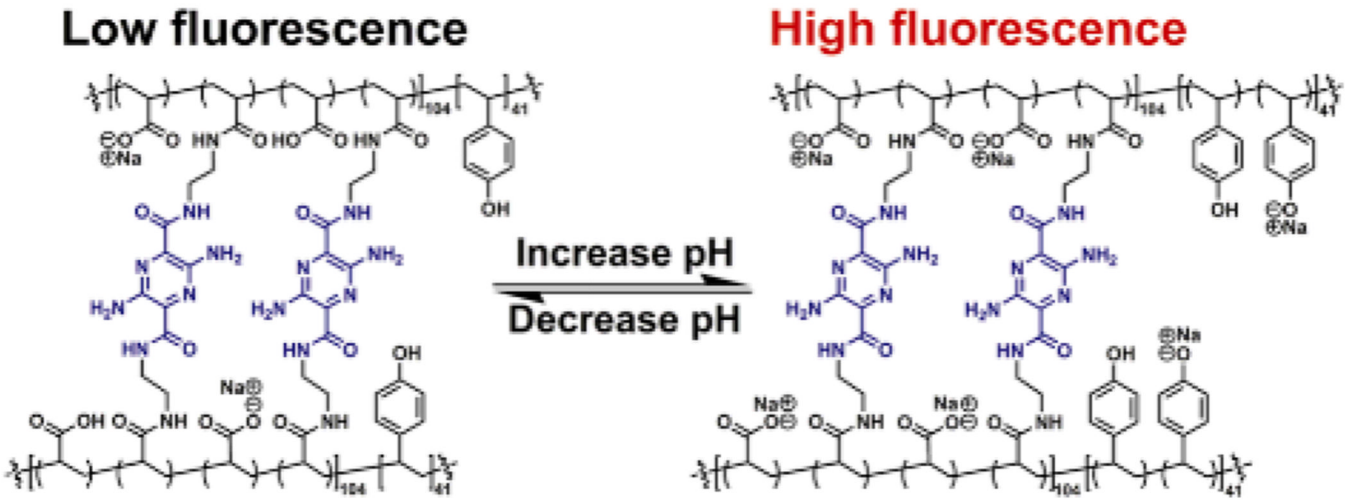

Figure 1.
Swelling/contraction of photonic SCKs as a function of pH.

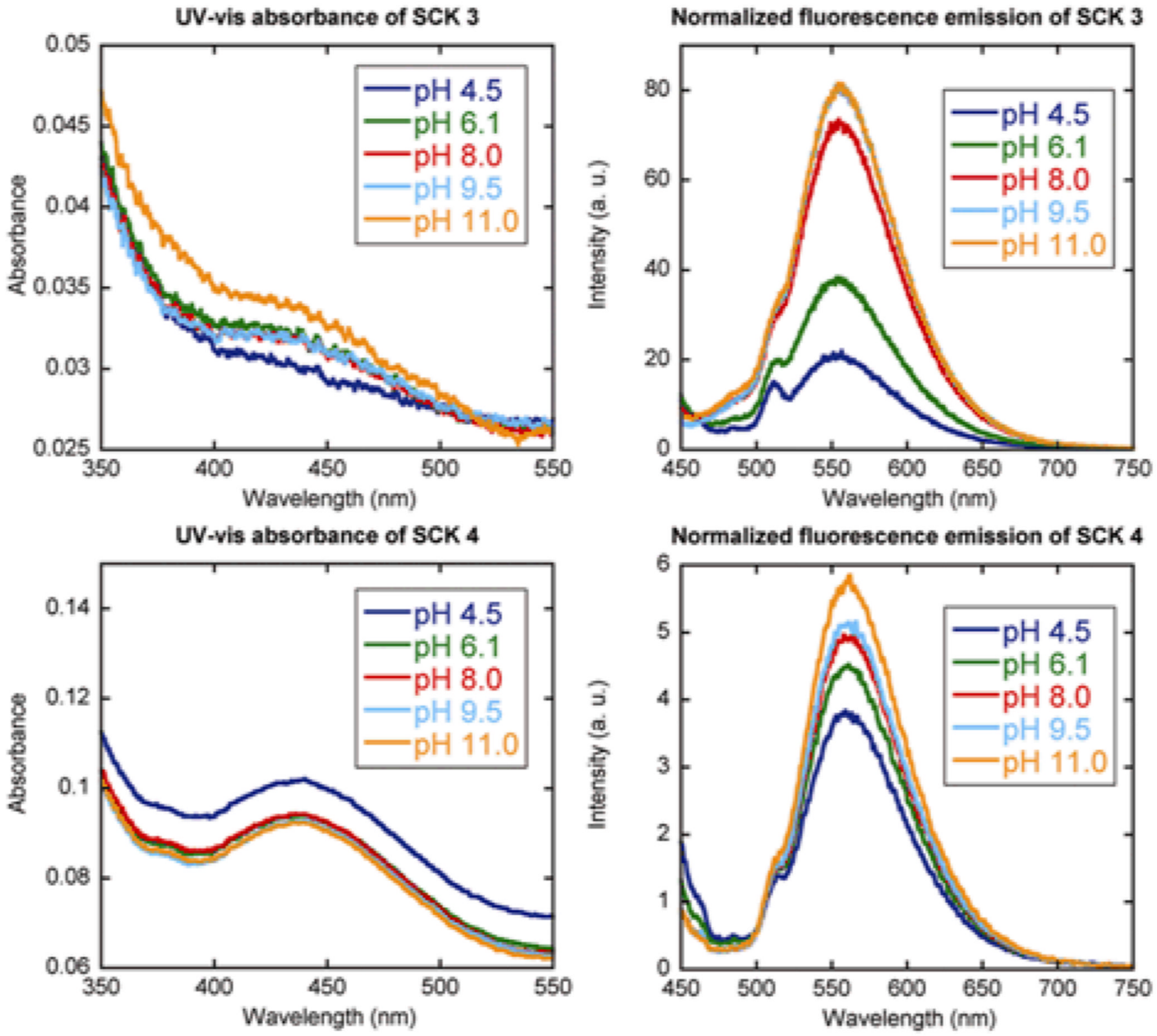

Figure 2.

UV-vis absorbance and normalized fluorescence emission of SCKs **3** and **4** as a function of pH and fluorophore loading (top: 6.25 mol% pyrazine relative to acrylic acid residues, bottom: 12.5 mol% pyrazine relative to acrylic acid residues.

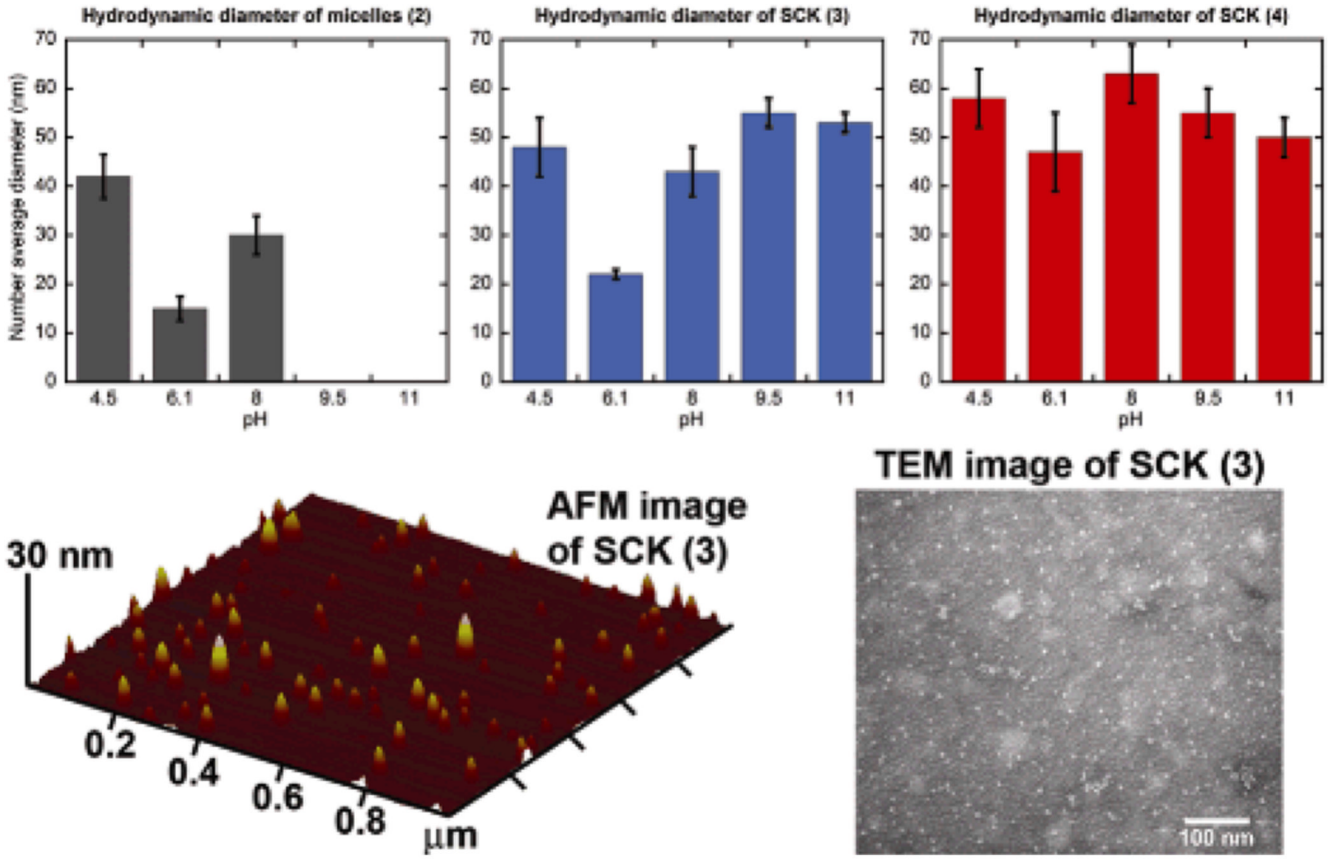

Figure 3.
Hydrodynamic diameter of **2** (left), **3** (middle), **4** (right) as a function of pH. AFM and TEM images of SCK **3** at pH 7.

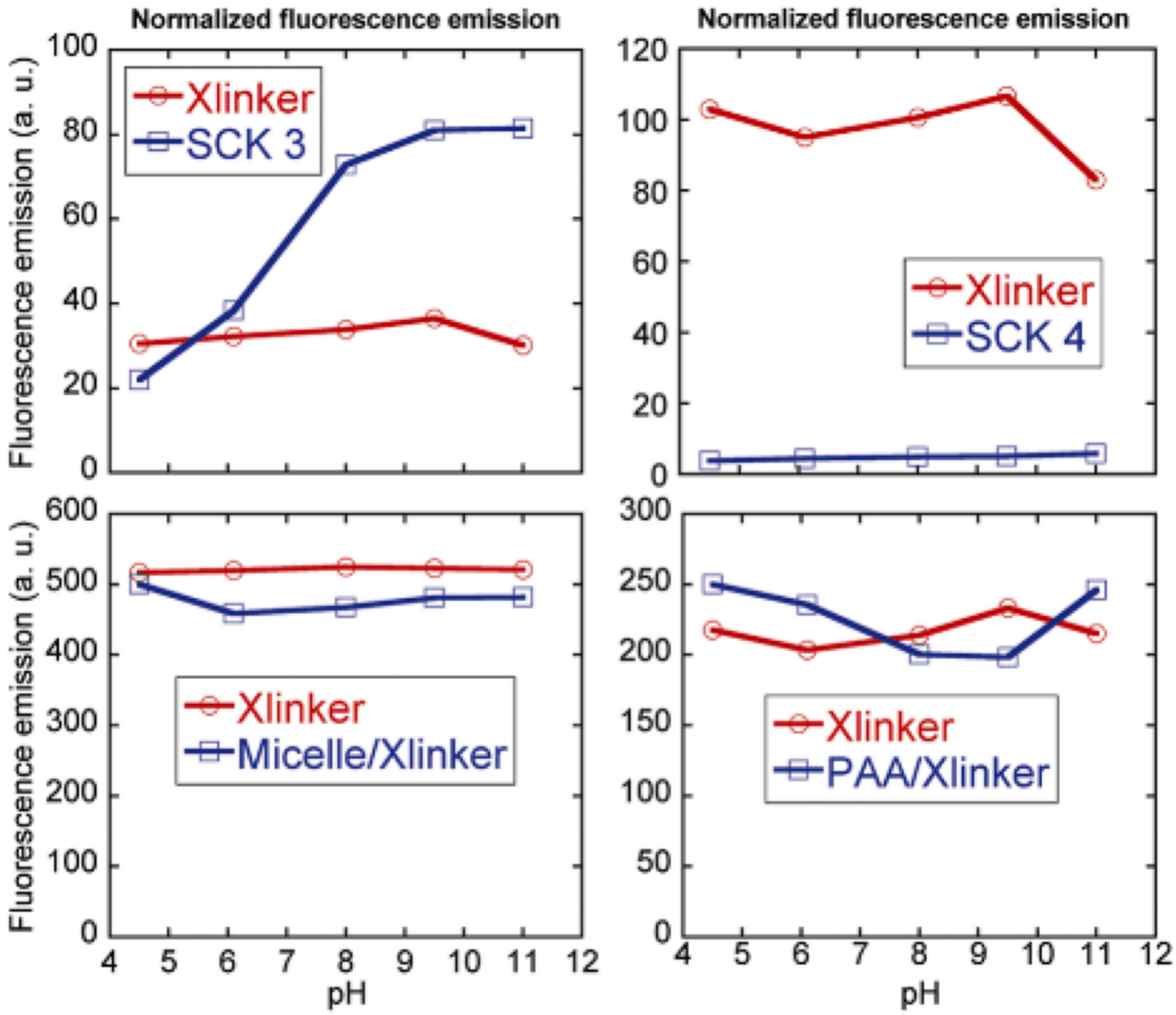

Figure 4.

Normalized fluorescence emission of SCK **3** and **4**, and mixtures of micelle/Xlinker, each as a function of pH. For each data set, the fluorescence intensity of the pyrazine is normalized by its concentration measured by UV-vis absorbance.

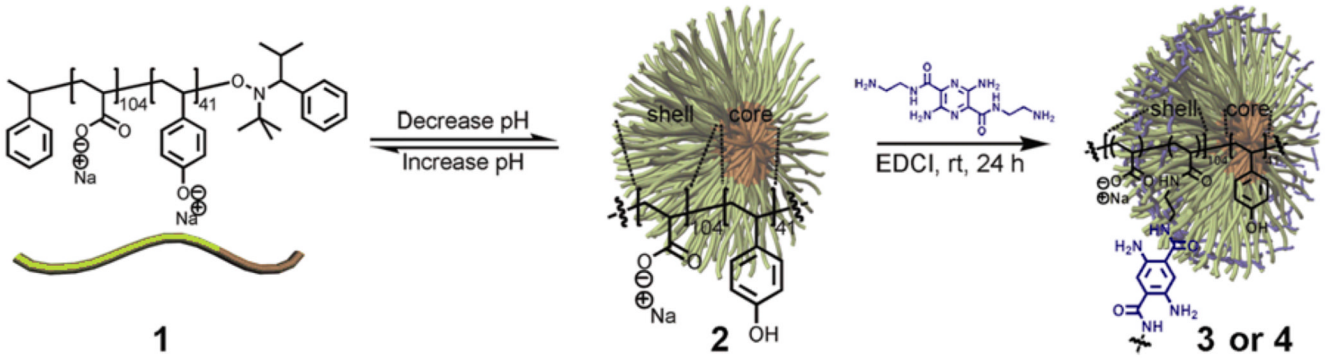

Scheme 1.

Assembly of micelles from poly(acrylic acid)-*b*-poly(*p*-hydroxystyrene) in water, with an adjustment of the solution pH, followed by the construction of pH-responsive SCKs upon shell crosslinking with fluorophores.

Adv Mater. Author manuscript; available in PMC 2011 November 4.

Table 1

Normalized percent change in fluorescence as a function of pH and fluorophore loading in SCK.

Solution pH	SCK 3[a]	SCK 4[b]	Micelle/ Xlinker[c]	PAA/ Xlinker[d]	Xlinker[e]
pH 4.5	100%	100%	100%	100%	100%
pH 6.1	180%	120%	92%	90%	100%
pH 8.0	330%	130%	93%	80%	100%
pH 9.5	370%	140%	96%	80%	110%
pH 11.0	370%	150%	96%	100%	100%

[a] 6.25 mol% fluorophore loading

[b] 12.5 mol% fluorophore loading

[c] 6.25 mol% fluorophore loading

[d] PAA and fluorophore complex at 6.25 mol% fluorophore loading, relative to acrylic acid residues

[e] fluorophore stock solution